HHS Public Access

Author manuscript

Biomater Sci. Author manuscript; available in PMC 2021 October 07.

Published in final edited form as:

Biomater Sci. 2020 October 07; 8(19): 5376–5389. doi:10.1039/d0bm00990c.

Transplantation of Insulin-like Growth Factor-1 Laden Scaffolds Combined with Exercise Promotes Neurovascular Regeneration and Angiogenesis in a Preclinical Muscle Injury Model

Cynthia A. Alcazar[1,2], **Caroline Hu**[2], **Thomas A. Rando**[2,3], **Ngan F. Huang**[2,4,5,*], **Karina H. Nakayama**[1,*]

[1]Department of Biomedical Engineering, Oregon Health & Science University, Portland, OR, USA

[2]Veterans Affairs Palo Alto Health Care System, 3801 Miranda Avenue, Palo Alto, CA, USA

[3]Department of Neurology and Neurological Sciences, Stanford University, Stanford, CA, USA

[4]Department of Cardiothoracic Surgery, Stanford University, Stanford, CA, USA

[5]The Stanford Cardiovascular Institute, Stanford University, CA, USA

Abstract

Skeletal muscle regeneration can be permanently impaired by traumatic injuries, despite the high regenerative capacity of skeletal muscle. Implantation of off-the-shelf engineered biomimetic scaffolds to the site of muscle injury to enhance muscle regeneration is an attractive therapeutic approach. Anisotropic nanofibrillar scaffolds provide spatial patterning cues to create organized myofibers, and growth factors such as insulin-like growth factor-1 (IGF-1) are potent inducers of both muscle regeneration as well as vascular regeneration. The aim of this study was to test the therapeutic efficacy of anisotropic IGF-1-releasing collagen scaffolds combined with voluntary exercise for the treatment of acute volumetric muscle loss, with a focus on histomorphological effects. To enhance the angiogenic and regenerative potential of injured murine skeletal muscle, IGF-1-laden nanofibrillar scaffolds with aligned topography were fabricated using a shear-mediated extrusion approach, followed by growth factor adsorption. Individual scaffolds released a cumulative total of 1244 ng ± 153 ng of IGF-1 over the course of 21 days *in vitro*. To test the bioactivity of IGF-1-releasing scaffolds, the myotube formation capacity of murine myoblasts was quantified. On IGF-1-releasing scaffolds seeded with myoblasts, the resulting myotubes formed were 1.5-fold longer in length and contained 2-fold greater nuclei per myotube, when compared to scaffolds without IGF-1. When implanted into the ablated murine tibialis anterior muscle, the IGF-1-laden scaffolds, in conjunction with voluntary wheel running, significantly increased the density of perfused microvessels by greater than 3-fold, in comparison to treatment with scaffolds

*To whom correspondence should be address: Dr. Karina H. Nakayama, PhD, Assistant Professor, Department of Biomedical Engineering, Oregon Health & Science University, Center for Health & Healing (CHH1), 3303 SW Bond Ave, Portland, OR 97239, Tel: 503 494-3081, Nakayaka@ohsu.edu; Dr. Ngan F. Huang, PhD, Assistant Professor, Department of Cardiothoracic Surgery, Stanford University, 300 Pasteur Drive, MC 5407, Stanford, CA 94305-5407, Tel: 650-849-0559, ngantina@stanford.edu.

Author Contributions: CA, TAR, NFH, and KHN designed and carried out experiments and analyzed data. CA, NFH, and KHN interpreted the results. CA and CH provided technical support for animal surgeries. CA and KHN wrote and organized the manuscript, with editorial input from NFH and TAR.

Conflicts of Interest

There are no conflicts of interest to declare.

without IGF-1. Enhanced myogenesis was also observed in animals treated with the IGF-1-laden scaffolds combined with exercise, compared to control scaffolds transplanted into mice that did not receive exercise. Furthermore, the abundance of mature neuromuscular junctions was greater by approximately 2-fold in muscles treated with IGF-1-laden scaffolds, when paired with exercise, in comparison to the same treatment without exercise. These findings demonstrate that voluntary exercise improves the regenerative effect of growth factor-laden scaffolds by augmenting neurovascular regeneration, and have important translational implications in the design of off-the-shelf therapeutics for the treatment of traumatic muscle injury.

Graphical Abstract

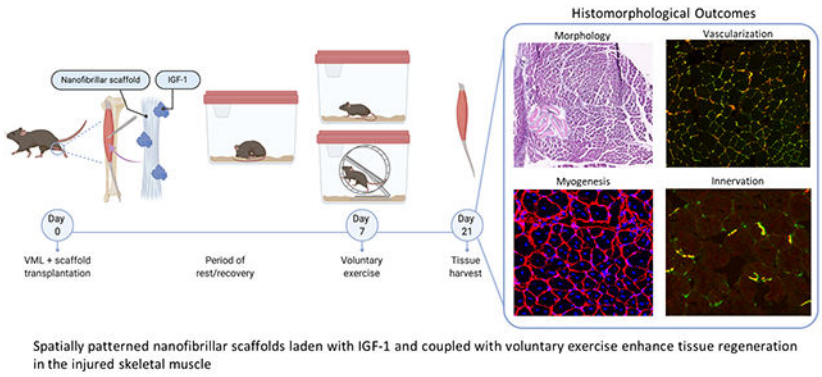

Spatially patterned nanofibrillar scaffolds laden with IGF-1 and coupled with voluntary exercise enhance tissue regeneration in the injured skeletal muscle

Keywords

angiogenesis; tissue engineering; muscle regeneration; vascular biology; regenerative medicine; rehabilitation; exercise

Introduction

Skeletal muscle exhibits a remarkable native ability to self-repair following injury. Extensive physical exercise and even minor muscle strains and tears induce a reparative response that involves activation of resident muscle stem cells to undergo proliferation and differentiation into fused myofibers to generate new muscle[1]. However, when trauma to the muscle results in severe damage to more than 20% of the tissue, the formation of compartmental tissue fibrosis out-paces the regenerative programs that would typically enable repair of the injury[2, 3]. Individuals are left with decreased muscle mass and impaired function. These traumatic skeletal muscle injuries are classified by the term volumetric muscle loss (VML) and are associated with patient disability due to the chronic loss of functional muscle structure and physiological mobility[4].

The current standard of care for patients with VML often involves repeated surgeries to debride scar tissue followed by transplantation of autologous muscle grafts[5]. When healthy adjacent muscle is insufficient due to severe trauma and nerve damage, free functional muscle transfer commonly of the latissimus dorsi or gracilis muscle is performed and often combined with neurorrhaphy[6, 7] However, these approaches frequently lead to donor site morbidities such as infection and necrosis resulting in graft failure[8]. A therapy that can

overcome these limitations would advance treatment approaches for this debilitating condition.

Experimental approaches to treat VML aim to restore muscle function through activation and mobilization of endogenous repair mechanisms or by engineering a biomimetic tissue ex vivo that can deliver supportive cells within a pro-regenerative niche to the site of muscle injury[9–11]. Our group has shown that an artificial niche could enhance engraftment and self-renewal of muscle stem cells following cardiotoxin-induced injury[12]. Using a bioconstruct designed to mimic the endogenous niche of muscle stem cells for the treatment of VML, we have reported restoration of function to injured muscle as well as neovascularization, myogenesis and innervation[13]. While cell-based tissue engineering approaches have demonstrated a range of success in regenerating muscle and restoring function[14, 15], one drawback is the dependence on cell source availability and the need to expand cells prior to therapeutic delivery. An alternative to cell-based muscle engineering is to stimulate regeneration of muscle *in situ* which largely relies on interactions between an acellular transplanted biomaterial and the host microenvironment. Successful outcomes are largely dictated by strategic engineering of material properties and oftentimes, benefiting from being coupled with small molecules or growth factors to assist with integration[16, 17].

Biomaterial design is a critical component in determining cell-matrix interactions. Tissue engineering commonly utilizes materials with controllable physical properties including porosity, stiffness, dimensionality, and spatial patterning[18]. The latter is a key element when engineering skeletal muscle which is highly ordered and contains longitudinally oriented myofibers that run in parallel bundles to maximize force contractions and control[19]. Cells interact with aligned fibers by taking on an elongated morphology parallel to the direction of the underlying fibers[20]. These physical cellular changes induce a range of cytoskeletal genetic programs involving increased expression of integrins and other matrix proteins[20–22]. Human adipose-derived stem cells as well as tendon-derived cells types including fibroblasts and progenitor cells have demonstrated increases expression of tendon-specific genes compared to randomly-oriented fibers[22–24]. Our group has demonstrated the ability of nanopatterned aligned scaffolds to enhance myogenic differentiation *in vitro* and myofiber regeneration and vascularization in vivo when coupled with myogenic and endothelial cells in a mouse skeletal muscle injury model[25].

Growth factors are key components of the regenerative niche and regulate the recruitment, survival, proliferation and differentiation of endogenous cells[26, 27]. An influential player in the skeletal muscle myogenic response is insulin-like growth factor-1 (IGF-1) which interacts with IGFBP-6 during the early stages of differentiation and promotes commitment of stem cells to lineage specific muscle cells[28, 29]. Studies using IGF-1 in combination with acellular biomaterial delivery vehicles, have demonstrated homing of host stem cells to the scaffold site when laden with IGF-1 thereby enhancing muscle regeneration in situ[16]. The incorporation of myogenic growth factors, specifically IGF-1 into acellular engineered materials is a promising approach for the generation of off the shelf therapeutics for the treatment of skeletal muscle injuries.

Following severe muscle injury, patients are often assigned physical rehabilitative therapy to better control physiological repair and expedite healing[30, 31]. We have previously demonstrated that physical exercise in a mouse VML model improves neurovascular regeneration when coupled to an acellular engineered scaffold[10]. Physical exercise stimulates the flow of blood to tissues and the extremities, aiding in capillarization by increasing the circulated endothelial progenitor cells, vascular endothelial growth factors (VEFG), tyrosine kinase-1, and matrix metalloproteinase[32]. Recently, it has also been shown that voluntary exercise has the capacity to rejuvenate quiescent muscle stem cells in old mice and accelerates muscle repair through the restoration of Cyclin D1 to youthful levels[33]. Accordingly, an engineered therapy that is coupled to voluntary exercise may produce a highly instructive and regenerative niche that is well suited to improve healing outcomes.

In the current study, we coupled rehabilitative exercise with IGF-1-laden nanofibrillar scaffolds for treatment of VML in a mouse model. To influence the homeostatic programs initiated during the initial rest/recovery period following injury, delivery of IGF-1 served to bridge this critical time during which the exercise-induced healing response is limited. Our findings show a therapeutic benefit based on histomorphology of both IGF-1 protein release as well as exercise in neuromuscular and vascular regeneration.

Results

IGF-1 Laden Scaffolds Enhance Myotube Formation in Vitro

To enhance the regenerative potential of injured skeletal muscle, IGF-1 laden nanopatterned scaffolds were fabricated from high concentration collagen type I using a previously described shear-based extrusion method[34, 35]. Scanning electron microscopy (SEM) imaging of scaffolds confirmed the high degree of orientation of aligned nanopatterned collagen fibrils with diameters between 50-100 nm [Figure 1A]. A 21 day timecourse measurement of IGF-1 protein released from scaffold bundles laden with IGF-1 showed a burst release of IGF-1 occurring within the first 24 hours followed by a gradual and more attenuated release of additional IGF-1 for a cumulative total of 1244 ng ± 153 ng of IGF-1 released *in vitro* by the scaffolds [Figure 1B, Supplementary Table 1].

To assess cellular interaction of the scaffolds with myogenic cells, C2C12 myoblasts were cultured on the scaffolds for 5 days under differentiation inducing conditions. After 5 days, staining of skeletal muscle myosin heavy chain-1 (MHC-1) was utilized to visualize mature myotubes and differences in myotube formation were apparent between the two groups. Myotubes that formed on scaffolds containing IGF-1 exhibited significantly longer lengths (339 ± 66 μm, $p<0.05$) and also greater number of nuclei per myotube (9.5 ± 1.7, $p<0.05$) compared to scaffolds without IGF-1 (204 ± 14 μm and 5.3 ± 0.4, respectively) [Figure 1C–1G].

Exercise Improves Neuromuscular Regeneration in Injured muscle

To assess the therapeutic efficacy, acellular scaffolds with or without IGF-1 were transplanted into the tibialis anterior (TA) muscles of mice immediately following volumetric muscle injury. After a rest period of 7 days, animals were then further subdivided

into exercise and non-exercise groups. The mice that were allowed to exercise on running wheels, were monitored for daily running activity as previously described[10, 13] [Figure 2A–B]. While the individual running habits of each mouse were highly variable, the daily running distances of mice that received control scaffolds compared to scaffolds with IGF-1 were not statistically different at baseline or at any given day throughout the duration of the 21 day period [Supplementary Table 2]. This indicates that mice assigned to the exercise group received similar levels of physical exercise. At 21 days following transplantation, the TA muscles were harvested and analyzed by hematoxylin & eosin staining. Staining showed minimal to no evidence of fibrosis near the scaffold interface with the muscle for any of the treatment groups [Figure 2C]. These data demonstrate that the nanopatterned collagen scaffolds do not elicit fibrosis.

The region of myogenesis was identified in TA cross-sections. All myofibers express the ECM protein, laminin, in their cellular membranes which enables visualization of the boundaries between individual myofibers. Regenerating myofibers exhibit centrally located nuclei and can be distinguished from non-regenerating myofibers, which have peripherally located nuclei [Supplementary Figure 1]. Extensive myofiber regeneration was observed in the 500 μm radial region adjacent to the transplanted scaffolds [Figure 3A]. Scaffolds with IGF-1 coupled with exercise stimulated enhanced myogenesis ($p < 0.05$) compared to control scaffolds without IGF-1 or exercise. Mice that were treated with the IGF-1-laden scaffolds combined with exercise had a density of 498 ± 39 myofibers/mm^2, compared to mice that received control scaffolds without exercise (343 ± 106 myofibers/mm^2) [Figure 3B]. However, despite a trend of improved myogenesis with the addition of exercise, the density of regenerating myofibers in mice treated with IGF-1 laden scaffolds without exercise (411 ± 42 myofibers/mm^2) was not statically different from animals that received exercise [Figure 3B]. Similarly, a trend of increased myogenesis is seen by scaffolds with IGF-1 compared to scaffolds without IGF-1; however, these differences were also not statistically significant.

Innervation of the injured TA muscle was assessed by staining of neuromuscular junctions. The abundance of mature neuromuscular junctions (NMJs) that co-expressed both alpha-bungarotoxin (acetylcholine receptors of neuromuscular junctions) and synaptophysin (presynaptic vesicles of neurons) was greater in muscles treated with IGF-1 laden scaffolds in conjunction with exercise (8.4 ± 1.8), in comparison to the same treatment without exercise (4.5 ± 1.4) ($p<0.05$) or control scaffolds without exercise (3.9 ± 2.4) ($p<0.01$) [Figure 3D]. However, without IGF-1, exercise did not affect apparent innervation of the TA muscle. Notably, IGF-1 laden scaffolds combined with exercise was the only treatment that resulted in significantly greater NMJ density ($p<0.01$) compared to control scaffolds without exercise, suggesting that exercise plays an integral role in the formation of neuromuscular junctions when coupled with growth factor laden scaffolds, which is consistent with our previous work[10, 13].

Scaffolds with IGF-1 Coupled with Exercise Enhance Re-vascularization

To assess vascular regeneration and anastomosis to the host circulation, isolectin, which binds to endothelial cells in contact with flowing blood, was infused via the tail vein on the

last day of the study. The co-staining of the isolectin conjugated to the fluorescent 647 probe with CD31 enabled histological visualization of actively perfused vasculature in the TA muscles. When implanted into the ablated murine TA muscle, the growth factor laden scaffolds in conjunction with voluntary caged wheel exercise significantly increased the density of isolectin+/CD31+ perfused microvessels by greater than 3-fold in comparison to treatment of constructs without IGF-1 [Figure 4A]. Whereas the perfused vessel density was 1256 ± 324 vessels/mm^2 for scaffolds containing IGF-1 with exercise, the density was 423 ± 467 vessels/mm^2 for scaffolds alone with exercise [Figure 4B]. Perfused vessel density was 918 ± 139 vessels/mm^2 in control tissue regions of non-regeneration. These differences could also be observed in longitudinal sections that show isolectin+ perfused blood vessels in parallel with endogenous muscle. Newly formed vessels near the transplanted scaffold were more dense and appear greater in length [Figure 4C]. Together, these findings suggest that aligned nanofibrillar scaffolds with IGF-1 release and coupled with an exercise regimen could be an effective treatment for traumatic muscle injury by enhancing innervation and vascular regeneration.

Discussion

Battlefield extremity wounds and fractures account for the majority (54–68%) of traumatic injuries experienced by United States military personnel engaged in the recent prolonged armed conflicts in the Middle East[36–38]. In particular, 53% of extremity injuries in Operation Iraqi Freedom and Operation Enduring Freedom were penetrating soft-tissue wounds which often require immediate life-saving treatment in the field followed by revascularization at a nearby hospital[39]. Despite advancements in medical interventions and an increase in forward-deployed assets that have reduced the number of war casualties, many of the injuries sustained will require multiple reconstructive surgeries and extensive rehabilitation. Single intervention, off-the-shelf therapies that can be paired with a mild to moderate rehabilitation regimen offer the potential for a more streamlined recovery.

The process of tissue regeneration involves several complex coordinated and simultaneous processes involving cell proliferation, homing of reparative cells to the injury site, re-vascularization, and re-innervation. The overall success of the therapy hinges on the ability to properly activate endogenous repair mechanisms by the host followed by functional integration. To tackle this complex challenge, a multi-faceted approach may provide the most robust and translationally feasible strategy.

Spatial patterning modulates skeletal muscle regeneration

We previously investigated the role of spatial patterning in tissue regeneration and demonstrated that an aligned topography of these scaffolds could beneficially modulate endothelial inflammatory phenotype as well as myogenic differentiation, maturation and function[10, 25, 34, 40]. Others have shown that electrospun scaffolds derived from synthetic materials such as polyglycolic acid (PGA), poly(lactic acid (PLA), and poly(lactic-co-glycolic acid) (PLGA) could be fabricated to possess anisotropy that induced spatial orientation of myoblasts along the fiber direction to facilitate more efficient fusion[41]. While synthetic materials are utilized for their controlled mechanical properties, natural

biomaterials such as collagen and fibrin have demonstrated varying degrees of either myogenic proliferation and differentiation and host integration[42]. In the current study, the spatially patterned aligned topography of the engineered scaffolds served to control cytoskeletal interactions through nano-scale guidance cues that directed cell orientation and organization along the longitudinal anatomy of the muscle. Although the precise mechanisms are still being established, the spatial guidance of these cells may enable more efficient fusion of myogenic cells into myofibers upon physical contact with the scaffold following injury/transplantation.

Regenerative approaches for the treatment of skeletal muscle injury

Regenerative approaches for treating VML span a wide range of biomaterials and engineering strategies. Some approaches utilize autologous minced muscle grafts to promote muscle regeneration and demonstrated partial functional recovery[15, 43, 44]. Our group has previously reported success in restoring structure and function to muscle tissue with both acute and chronic models of VML injury using a natural scaffold with muscle stem cells and muscle resident cells[13]. De novo innervation of regenerated myofibers and further enhancement of force production were observed when these bioconstructs were paired with an exercise regimen[13]. Similarly, in our previous work with anisotropic nanofbrillar scaffolds, we demonstrated muscle regeneration and neovascularization when these scaffolds were transplanted with both myogenic cells and endothelial cells[25]. However, a key limitation of these approaches is the tissue source availability which hinders the translational feasibility of this method over autologous grafting. Nonetheless, it provides a useful benchmark for ex vivo engineered tissues as the treatment contains a mix of cells already native to the muscle.

An ideal strategy might not require all of the native cell populations for meaningful regeneration to occur. Another approach involves a combinatorial strategy that partners engineered biomaterials with cells and growth factors to create an optimized niche to modulate the regenerative response. Keratin, a naturally occurring extracellular matrix material[45] was made into hydrogels and were used in combination with insulin-like growth factor-1 (IGF-1) and basic fibroblast growth factor (bFGF) to deliver skeletal muscle progenitor cells to the site of muscle injury. Interestingly, the group that performed the best in terms of recovery of contractile force and histological analysis for new muscle formation was acellular and contained only the materials laden with growth factors[45]. These findings highlight the potential for a scaffold to have a greater regenerative effect without cells compared to when cells are incorporated into the treatment.

Biomechanical stimulation and scaffold delivery of IGF-1 in skeletal muscle regeneration

Biomaterials designed to modulate regeneration without the support of transplanted cells often are coupled with assistive biomimetics to enhance the endogenous reparative response. Incorporation of IGF-1 into scaffolds, served to stimulate proliferation and initiation of myogenic fusion of skeletal muscle myoblasts *in vitro* and likely aided in the activation of resident stem cells and recruitment of endogenous endothelial cells to the scaffold and injury site[16, 26, 28, 29]. Circulating IGF-1 is positively correlated with improved health parameters such as cardiovascular health and muscle endurance[46]. Although physiological levels of

IGF-1 in the muscle tissue and blood circulation were not evaluated in the current study, we expect a majority of delivered IGF-1 to be localized to the ablated tissue region with progressively decreasing concentrations correlating with increasing radial distance from the injury site. While local delivery of 0.9μg of IGF-1 through a subcutaneous miniosmotic pump into rat TA was shown to have a measurable impact on the amount of circulating IGF[47], our scaffold's 3-dimensional architecture and volume are restricted by the dimensions of the ablated muscle and subsequently is a limitation in the diffusion of IGF-1 beyond the injury site. Although it is anticipated that IGF-1 delivered by the scaffold would not significantly impact circulating IGF-1 levels, the effects on regional tissue regeneration is maximized through the local retention of IGF-1 to the ablated region. The IGF-1 gene is normally activated in response to mechanical stimulation produced by repeated cyclical stretch[48] and without normal cycles of tension and stretch, this pathway sits inactive leading to muscle atrophy[49] and thereby underscores the importance of physical exercise in muscle health and healing. However, patients recovering from VML require rest during the initial phases of healing and therefore, mechanical stimulation to induce production of endogenous IGF-1 is not possible. To replicate this recovery period of inactivity in our mouse model, the introduction of exercise was similarly delayed by 1 week. To compensate for the lack of mechanical stimulation during the initial stages of healing, patterned scaffolds were used to deliver IGF-1 to the site of muscle injury. The rationale is that a local burst delivery of exogenous IGF-1 to the injury site would help bridge this critical period of mechanical inactivity by initiating a pro-regenerative program earlier in the healing timeline when the body is not producing IGF-1 through rigorous mechanical stimulation. Others have demonstrated the benefits of a bolus delivery of combined IGF-1 and VEGF into an ischemic hindlimb injury in mice which led to enhance muscle size and limb vascularization despite 80% of IGF-1 being released within the first 24 hours[50]. They also showed that this approach could enhance early regeneration of damaged neuromuscular junctions, which is consistent with our findings and indicates that bolus growth factor delivery can promote regenerative programs earlier in the healing process.

Matching of the release kinetics of growth factor-loaded scaffolds with the timing of endogenous healing programs has been shown to enhance regenerative outcomes. Injectable materials such as alginate hydrogel[51] and (PEG)ylated fibrin gel[52] have been used to deliver IGF-1 for the treatment of myocardial infarction and tourniquet induced ischemia/reperfusion in hindlimbs, respectively. These studies both demonstrated an initial burst release of approximately half (50-65%) of IGF-1 within the first 6 hours with attenuated release of a majority (~90%) of remaining IGF-1 within 24 hours. The IGF-1 laden scaffolds used in the current study exhibit similar release kinetics and further studies are needed to explore optimal approaches for prolonged growth factor release in injury models. However, while the majority of IGF-1 protein was released from the scaffolds in the first 24 hours (approximately 1200 micrograms), even picogram levels of IGF-1 treatment to injured cardiac muscle has been shown to be sufficient in promoting angiogenesis following a myocardial infarction in a rat model[53]. Therefore, it is reasonable that even the nanogram levels of IGF-1 that were being delivered by the scaffold towards the end of the 21 day study period likely continued to contribute to a pro-regenerative healing program.

Enhancing skeletal muscle regeneration through running exercise

The pairing of these scaffolds with physical exercise was intended to stimulate blood flow to the site of injury and to enhance production of myogenic and angiogenic growth factors. Exercise not only aids in the formation of de novo vasculature but may also play a role in mediating fibrosis and enhancing innervation through stabilization of nerve ingrowth[13, 54–56]. Furthermore, exercise has been shown to mobilize a reserve of resident muscle satellite cells to initiate the process of regenerating damaged muscle[57]. Mouse models that integrated voluntary endurance training using treadmill-based exercise, demonstrated increased levels of satellite cell production[13, 58, 59]. The exercise regimen that was implemented in the current study involved an initial period of rest followed by two weeks of voluntary exercise. Previous studies from our group assessed the time required for mice that underwent VML injury to recover normal running patterns consistent with uninjured control mice[13]. Running performance recovery was achieved 7 days following initial VML injury. Additionally, introduction of exercise earlier than 7 days delayed muscle regeneration and promoted the formation of fibrotic tissue whereas delayed exercise accelerated myogenesis and attenuated fibrosis[13]. Therefore, a regimen consisting of a 7 day recovery period, followed by 2 weeks of voluntary running was adopted. For clinical cases of skeletal muscle injury, when eccentric and concentric exercise was incorporated into a recovery regimen, a physiological response was stimulated by satellite cell activity to promote skeletal muscle production[60] compared to individuals who remained static[61].

Combinatorial approaches for enhancing regeneration in injured muscle

In our studies, exercise played a decisive role in enhancing the formation of mature neuromuscular junctions when IGF-1 was also delivered with the scaffolds; however, without the presence of exogenous IGF-1, exercise-based neuromuscular junction density was not enhanced. Our findings suggest a synergy between voluntary exercise and IGF-1 delivery in which the combined application of both were necessary to promote enhanced re-innervation. Similarly, IGF-1 alone was not sufficient to enhance vascularization of the injured tissue; however, when IGF-1 was coupled with exercise, greater perfused vascular densities were observed compared to scaffolds delivered without IGF-1 and treated with exercise. This synergy could be in part due to the sequential activation of regenerative programs by exogenously delivered IGF-1 early in the healing process followed by mechanical stimulation of endogenous IGF-1 production through exercise later in the healing regimen. While high intensity exercise and endurance training are associated with increased circulating levels of IGF-1[62, 63] as well as increased levels of IGFBP-1 and IGFBP-3[62, 63], a small study with healthy men reported decreased levels of circulating IGF-1 following low-intensity aerobic training and an increase of 16% of IGFBP-1[64] suggesting that there is a threshold of physical activity associated with IGF-1 and IGFBP production. Additional studies are needed to determine the mechanisms involved in this process and the functional relationship of exercise and IGF-1 in skeletal muscle healing and regeneration.

Taken together, our three-pronged approach supported more efficient myogenesis *in vitro* and enhanced neurovascular tissue regeneration in vivo. These findings highlight the importance of using both engineering and physiological approaches to create an optimal

regenerative niche in which a combinatorial treatment is more effective than the sum of its parts.

Materials and Methods

Generation of Parallel-Aligned Nanofibrillar Collagen Scaffolds

Aligned nanofibrillar collagen scaffolds were fabricated as described previously[10, 25, 40]. Briefly, rat-tail collagen-type I (10 mg/mL in 0.02 N in acetic acid, pH 3.5, Corning) was dialyzed to 30 mg/mL using a semi-permeable cellulose dialysis tubing of pore size 32 x 20.4 mm (ThermoFisher) and polyethylene glycol (Sigma) at 4°C. The aligned nanofibrillar collagen scaffold strip (approximately 25mm x 1mm) was extruded from a 22G blunt tip needle onto glass slides at a velocity of 340 mm/s, while submerged within warmed 10X phosphate buffered saline (PBS, pH 7.4) at 37°C to initiate fibrillogenesis. The nanostructure and fibril alignment of the scaffolds were visualized by routine scanning electron microscopy (SEM), as described previously[34].

To create a 3D scaffold bundle, 8 scaffold strips were assembled in parallel with dimensions that were 9mm x 2mm x 3mm. Scaffolds were allowed to dry overnight in a laminar flow hood and were sterilized with 70% ethanol prior to use followed by several washes with sterile 1X PBS. Growth factor laden scaffolds were generated by incubation of dehydrated scaffolds with 250 μg/mL recombinant human IGF-1 (Peprotech) diluted in 0.1% bovine serum albumin (BSA) at 37°C and 5% CO_2 overnight. Control scaffolds were incubated in 0.1% BSA overnight.

Characterization of IGF release

To assess the rate of IGF-1 release from scaffolds (N=4) over time, IGF-1-laden scaffolds were incubated in 0.1% BSA at 37°C and the supernatant was collected over 21 days on days 0 (4h and 8h), 1, 2, 4, 7, 14, and 21. IGF-1 concentration was quantified by enzyme linked immunosorbent assay (ELISA) using a Human IGF-1 Quantikine ELISA kit (R&D systems) following manufacturer's instructions. Readings were taken at 10 minutes following addition of the stop solution at a wavelength of 450nm with correction at 540nm.

Cellular Interaction with Myoblasts

Scaffolds (N=4) with or without IGF-1 were seeded with C2C12 myoblasts (ATCC) at a concentration of 500,000 cells/scaffold in a differentiation medium that consisted of DMEM (Gibco) with 3% horse serum and 1% penicillin/streptomycin. Samples were fixed following 5 days of differentiation in 4% paraformaldehyde (Alfa Aesar), washed with 1X PBS, and then stored at 4°C until use.

Immunofluorescence Staining

Immunofluorescent staining was performed on samples to visualize cellular interactions with the scaffolds. Samples were permeabilized in 0.5% Triton-X100 (Sigma) and blocked with 1% BSA (Sigma). All subsequent dilutions were performed using 0.1% BSA for antibody preparation. For assessment of myotube morphology and maturity, fixed samples were incubated with a primary antibody against myosin heavy chain (MHC, Abcam) for 16h

at 4°C followed by Alexa Fluor-594 or −488 antibody (Life Technologies). Images were acquired using a Zeiss LSM710 confocal microscope.

Quantification of Myotube Morphology and Maturity

Myoblasts were cultured on scaffolds with or without IGF-1. To assess the impact of the release of IGF-1 on myoblast differentiation, myotube length, density of myotubes, and nuclei per myotube (n=4 each group) were fixed on Day 5 and stained for fast myosin heavy chain marker (MHC, Abcam) as described above. Samples were acquired using a Zeiss LSM710 confocal microscope and z-stacked (100-200μm stack) tile-stitched (7x2 frames) 20X images were taken. The total ROI area of a single tile-stitched composite image was 9492.18 x 2761.97 μm or roughly 9.5 mm x 2.8 mm which accounts for the entire scaffold area and hence a single ROI captured the full length and width of the scaffold (for reference, the transplanted scaffolds were cut to fit the muscle defect to a which was approximately 7 mm x 3 mm x 2 mm). Using the line and multipoint tools in ImageJ64, myotube length and nuclei per myotube were measured, respectively. Myotubes were defined as elongated MHC + structures and containing ≥ 3 nuclei per myotube.

Transplantation of IGF-1 Scaffolds into a VML Mouse Model

All animal procedures were performed in accordance with the Guidelines for Care and Use of Laboratory Animals of the Veterans Affairs Palo Alto Health Care System (VAPAHCS) and approved by the Institutional Animal Care and Use Committee at the VAPAHCS. 129S1/SvlmJ male mice (8-10 weeks old) obtained from Jackson Laboratories were anesthetized and maintained with 1-3% Isoflurane and an oxygen flow rate of 1 L/min. The mice were administered an analgesic and antibiotic, Buprenorphine slow release (0.6 - 1.0 mg/kg) and Baytril (5 mg/kg), respectively. Animals were maintained at the Veterinary Medical Unit at VAPAHCS in group housing, unless they received the voluntary cage wheel running treatment in the singly housed cage systems. Water and a standard rodent diet were given ad libitum. At the end of the 21 day study, animals were euthanized with Isoflurane overdose, and cervical dislocation was performed as a secondary form of euthanasia.

For in vivo studies, acellular nanofibrillar scaffolds with or without IGF-1 were transplanted into a mouse model of acute volumetric muscle loss (VML) that was created by the surgical excision of 40% of the anterior tibialis (TA) muscle. This model has been described previously[13] and involves the creation of a muscle defect approximately 7 mm x 2 mm x 3 mm. Constructs were sutured at the distal and proximal ends of the defect followed by suture closure of the muscle and skin flaps. After receiving scaffolds with or without IGF-1, animals were subdivided into groups that received exercise and those that were returned to standard housing for a total of 4 treatment groups: 1) Scaffold without Exercise(n=4 TAs); 2) Scaffold + IGF-1 without Exercise (n=4 TAs); 3) Scaffold with Exercise, (n=4 TAs); 4) Scaffold + IGF-1 with exercise, (n=6 TAs).

Animal Exercise Regimen

Baseline running distances were recorded for all mice, followed by random distribution into one of the 4 treatment groups (n=4 TAs for each group except n=6 for the scaffold+IGF-1 with exercise group). Exercised animals were introduced to cage wheels for 72 hours prior to

VML surgeries and allowed to acclimate to single housing conditions. To minimize distress animal cages were kept in close visual proximity to each other and were partitioned in an isolated area to minimize traffic. Following transplantation, animals were allowed to recover in traditional housing cages for 7 days with their original littermates, after which, animals were either transferred to individual cages containing cage wheels (Scurry Mouse running Wheel 80820S, Lafayette Instrument) or remained in their standard group housing for 14 days. Running activity was digitally recorded at 3 second intervals by computer-assisted counters (Scurry mouse activity counter 86110, Lafayette Instrument), and data was collected and analyzed using the Scurry Activity Monitoring Software v17.10 (Lafayette Instrument). Running distance was binned in 15 minute intervals for monitoring daily activity.

Histological Analysis of Muscle Regeneration and Innervation

On day 21 following initial VML, the tail veins were injected with 200 μl of isolectin (GS-IB4 from Griffonia simplicifolia, Alexa Fluor 647 conjugate, Invitrogen, 50μg/ml), a fluorescently labeled endothelial binding protein and the TA muscle was extracted and processed for histological analysis. Serial transverse cryosections (10 μm thickness) of the TA muscle were stained with hematoxylin and eosin (H&E) to examine tissue morphology. To quantify myofiber regeneration within the scaffold's immediate vicinity (within 500 μm from the scaffold's borders), muscle tissue cryosections were immunofluorescently stained with Laminin (Abcam) and tiled z-stacked images (5×5 montages using 20X objectives) were taken using confocal microscopy to capture the entire cross-section of the tissue. Using the multipoint tool in ImageJ, the total number of regenerating myofibers, defined as myofibers with centrally located nuclei, in the vicinity of the scaffold implants (defined as 500 μm from the scaffold periphery) was counted (n=4 for each group except n=6 for the scaffold+IGF-1 with exercise group).

Immunofluorescent staining of neuromuscular junction markers, α-bungarotoxin (Invitrogen) and synaptophysin (Sigma) was performed to quantify muscle innervation. Confocal tiled images from transverse cryosections were reconstructed to enable visualization of the TA muscle cross-section for each animal (n=4 for each group except n=6 for the scaffold+IGF-1 with Exercise group). The number of α-bungarotoxin$^+$ and synaptophysin$^+$ neuromuscular junctions were quantified to give the mature neuromuscular junction density (# α-bungarotoxin$^+$/synaptophysin$^+$ junctions per square millimeter). The density of total neuromuscular junctions was defined as the # α-bungarotoxin$^+$ junctions per square millimeter of muscle tissue).

Immunofluorescent Staining and Assessment of Blood Perfusion

On day 21 after implantation, animals were injected via the tail vein with 100μl (1mg mL-1) of endothelial-binding fluorescent isolectin GS-IB4 (Invitrogen) before euthanasia, and the TA muscle was explanted. The TA muscles were fixed in 0.4% paraformaldehyde at 4°C for 16 hours followed by density equilibration in 20% sucrose for 2-3 hours and embedding for cryosectioning of tissue sections in the transverse or longitudinal planes. Histological quantification of blood perfusion was performed by immunofluorescence staining of endothelial marker, CD31 (R&D Systems). Five non-overlapping images (500 μm x 500 μm)

from transverse cryosections for each animal (n=4 for each group except n=6 for the scaffold +IGF-1 with Exercise group) were taken within 500 μm from the transplanted scaffolds. The CD31+ vessels that co-stain with isolectin indicated vessels suggest functional anastomosis to the host circulation and were quantified to give the perfused vessel density (expressed as the total number of perfused vessels per square millimeter). Control values of vascular density were obtained by quantification of CD31+/isolectin+ vessels located in the outermost non-regenerating regions of 4 representative TA tissues (3 images per tissue). Longitudinal sections were also imaged using confocal microscopy for isolectin to determine qualitative global organization of regenerating vasculature adjacent to the scaffold.

Statistical Analysis

All graphs were made in either Microsoft Excel or GraphPad PRISM and display mean ± standard deviation (SD). Statistical analysis was performed using Graph Pad PRISM software. Where appropriate, a one-way ANOVA was performed with post hoc Tukey's adjustment. For comparison between two groups only, a student's two-tailed unpaired t-test was used. Significance was taken at $p \leq 0.05$ (*), $p \leq 0.01$ (**).

Conclusions

There is an expanding health care demand for off-the-shelf therapeutics to treat traumatic musculoskeletal injuries. Acellular biomaterials that have the ability to modulate the regenerative niche hold great potential to alleviate the treatment burden and morbidity prognosis for patients who experience these debilitating conditions. In this study we demonstrated that a nanofibrillar scaffold with aligned topography coupled with IGF-1 could enhance regeneration in a volumetric muscle injury when paired with voluntary exercise. The simple design of the material combined with a common patient post-recovery regimen imparts a streamlined and accessible approach for this regenerative therapeutic. These findings highlight how health outcomes can be positively controlled through combinatorial engineering approaches and physical medicine.

Supplementary Material

Refer to Web version on PubMed Central for supplementary material.

Acknowledgments

This research received funding from the Alliance for Regenerative Rehabilitation Research & Training (AR3T), which is supported by the Eunice Kennedy Shriver National Institute of Child Health and Human Development (NICHD), National Institute of Neurological Disorders and Stroke (NINDS), and National Institute of Biomedical Imaging and Bioengineering (NIBIB) of the National Institutes of Health under Award Number P2CHD086843. This study was supported by grants to N.F.H. from the US National Institutes of Health (R01 HL127113, and R01 HL142718), the National Science Foundation (1829534), and the Department of Veterans Affairs (1I01BX002310 and 1I01BX004259). This work was also supported by grants to T.A.R from the National Institutes of Health (P01 AG036695), the California Institute of Regenerative Medicine, the Department of Defense, and the Department of Veterans Affairs (REAP and RR&D Merit Reviews). This study was also supported by grants to K.H.N. from the National Institutes of Health (4R00HL136701–03) and AR3T (CNVA00048860).

References

1. Scharner J, Zammit PS. The muscle satellite cell at 50: the formative years. Skeletal muscle. 2011;1(1):28. [PubMed: 21849021]
2. Corona BT, Wenke JC, Ward CL. Pathophysiology of volumetric muscle loss injury. Cells Tissues Organs. 2016;202(3-4):180–8. [PubMed: 27825160]
3. Turner NJ, Badylak SF. Regeneration of skeletal muscle. Cell and tissue research. 2012;347(3):759–74. [PubMed: 21667167]
4. Garg K, Ward CL, Hurtgen BJ, Wilken JM, Stinner DJ, Wenke JC, et al. Volumetric muscle loss: persistent functional deficits beyond frank loss of tissue. Journal of Orthopaedic Research. 2015;33(1):40–6. [PubMed: 25231205]
5. Klinkenberg M, Fischer S, Kremer T, Hernekamp F, Lehnhardt M, Daigeler A. Comparison of anterolateral thigh, lateral arm, and parascapular free flaps with regard to donor-site morbidity and aesthetic and functional outcomes. Plastic and reconstructive surgery. 2013;131(2):293–302. [PubMed: 23357991]
6. Stevanovic MV, Cuéllar VG, Ghiassi A, Sharpe F. Single-stage reconstruction of elbow flexion associated with massive soft-tissue defect using the latissimus dorsi muscle bipolar rotational transfer. Plastic and Reconstructive Surgery Global Open. 2016;4(9).
7. Li MTA, Willett NJ, Uhrig BA, Guldberg RE, Warren GL. Functional analysis of limb recovery following autograft treatment of volumetric muscle loss in the quadriceps femoris. Journal of biomechanics. 2014;47(9):2013–21. [PubMed: 24280565]
8. Lin C-H, Lin Y-T, Yeh J-T, Chen C-T. Free Functioning Muscle Transfer for Lower Extremity Posttraumatic Composite Structure and Functional Defect. Plastic and Reconstructive Surgery. 2007;119(7):2118–26. [PubMed: 17519710]
9. Nakayama KH, Shayan M, Huang NF. Engineering Biomimetic Materials for Skeletal Muscle Repair and Regeneration. Advanced Healthcare Materials. 2019;8(5):1801168.
10. Nakayama KH, Alcazar C, Yang G, Quarta M, Paine P, Doan L, et al. Rehabilitative exercise and spatially patterned nanofibrillar scaffolds enhance vascularization and innervation following volumetric muscle loss. NPJ Regenerative medicine. 2018;3:16-. [PubMed: 30245849]
11. Hurtgen BJ, Ward CL, Leopold Wager CM, Garg K, Goldman SM, Henderson BEP, et al. Autologous minced muscle grafts improve endogenous fracture healing and muscle strength after musculoskeletal trauma. Physiological Reports. 2017;5(14):e13362. [PubMed: 28747511]
12. Quarta M, Brett JO, DiMarco R, De Morree A, Boutet SC, Chacon R, et al. An artificial niche preserves the quiescence of muscle stem cells and enhances their therapeutic efficacy. Nature biotechnology. 2016;34(7):752–9.
13. Quarta M, Cromie M, Chacon R, Blonigan J, Garcia V, Akimenko I, et al. Bioengineered constructs combined with exercise enhance stem cell-mediated treatment of volumetric muscle loss. Nature Communications. 2017;8(1):1–17.
14. Lesman A, Koffler J, Atlas R, Blinder YJ, Kam Z, Levenberg S. Engineering vessel-like networks within multicellular fibrin-based constructs. Biomaterials. 2011;32(31):7856–69. [PubMed: 21816465]
15. Goldman SM, Henderson BEP, Walters TJ, Corona BT. Co-delivery of a laminin-111 supplemented hyaluronic acid based hydrogel with minced muscle graft in the treatment of volumetric muscle loss injury. PLOS ONE. 2018;13(1):e0191245. [PubMed: 29329332]
16. Ju YM, Atala A, Yoo JJ, Lee SJ. In situ regeneration of skeletal muscle tissue through host cell recruitment. Acta Biomaterialia. 2014;10(10):4332–9. [PubMed: 24954910]
17. Badylak SF, Dziki JL, Sicari BM, Ambrosio F, Boninger ML. Mechanisms by which acellular biologic scaffolds promote functional skeletal muscle restoration. Biomaterials. 2016;103:128–36. [PubMed: 27376561]
18. Jenkins TL, Little D. Synthetic scaffolds for musculoskeletal tissue engineering: cellular responses to fiber parameters. NPJ Regenerative medicine. 2019;4(1):1–14. [PubMed: 30622740]
19. Takahashi H, Shimizu T, Okano T. Engineered Human Contractile Myofiber Sheets as a Platform for Studies of Skeletal Muscle Physiology. Scientific Reports. 2018;8(1):13932. [PubMed: 30224737]

20. Whited BM, Rylander MN. The influence of electrospun scaffold topography on endothelial cell morphology, alignment, and adhesion in response to fluid flow. Biotechnol Bioeng. 2014;111(1):184–95. [PubMed: 23842728]
21. Lee NM, Erisken C, Iskratsch T, Sheetz M, Levine WN, Lu HH. Polymer fiber-based models of connective tissue repair and healing. Biomaterials. 2017;112:303–12. [PubMed: 27770633]
22. Yin Z, Chen X, Chen JL, Shen WL, Nguyen TMH, Gao L, et al. The regulation of tendon stem cell differentiation by the alignment of nanofibers. Biomaterials. 2010;31(8):2163–75. [PubMed: 19995669]
23. Cheng X, Tsao C, Sylvia VL, Cornet D, Nicolella DP, Bredbenner TL, et al. Platelet-derived growth-factor-releasing aligned collagen–nanoparticle fibers promote the proliferation and tenogenic differentiation of adipose-derived stem cells. Acta biomaterialia. 2014;10(3):1360–9. [PubMed: 24291329]
24. Wu S, Peng H, Li X, Streubel PN, Liu Y, Duan B. Effect of scaffold morphology and cell co-culture on tenogenic differentiation of HADMSC on centrifugal melt electrospun poly (L-lactic acid) fibrous meshes. Biofabrication. 2017;9(4):044106. [PubMed: 29134948]
25. Nakayama KH, Quarta M, Paine P, Alcazar C, Karakikes I, Garcia V, et al. Treatment of volumetric muscle loss in mice using nanofibrillar scaffolds enhances vascular organization and integration. Communications biology. 2019;2:170-. [PubMed: 31098403]
26. Florini JR, Ewton DZ, Coolican SA. Growth hormone and the insulin-like growth factor system in myogenesis. Endocrine reviews. 1996;17(5):481–517. [PubMed: 8897022]
27. Duan C, Ren H, Gao S. Insulin-like growth factors (IGFs), IGF receptors, and IGF-binding proteins: roles in skeletal muscle growth and differentiation. General and comparative endocrinology. 2010;167(3):344–51. [PubMed: 20403355]
28. Aboalola D, Han VK. Different effects of insulin-like growth Factor-1 and insulin-like growth Factor-2 on myogenic differentiation of human mesenchymal stem cells. Stem Cells International. 2017;2017.
29. Florini JR, Ewton DZ, Roof SL. Insulin-like growth factor-I stimulates terminal myogenic differentiation by induction of myogenin gene expression. Molecular Endocrinology. 1991;5(5):718–24. [PubMed: 1649394]
30. Tidball JG. Inflammatory processes in muscle injury and repair. American Journal of Physiology-Regulatory, Integrative and Comparative Physiology. 2005;288(2):R345–R53.
31. Baoge L, Van Den Steen E, Rimbaut S, Philips N, Witvrouw E, Almqvist K, et al. Treatment of skeletal muscle injury: a review. ISRN orthopedics. 2012;2012.
32. Ross MD, Wekesa AL, Phelan JP, Harrison M. Resistance exercise increases endothelial progenitor cells and angiogenic factors. Medicine & Science in Sports & Exercise. 2014;46(1):16–23. [PubMed: 24346188]
33. Brett JO, Arjona M, Ikeda M, Quarta M, de Morrée A, Egner IM, et al. Exercise rejuvenates quiescent skeletal muscle stem cells in old mice through restoration of cyclin D1. Nature Metabolism. 2020;2(4):307–17.
34. Nakayama KH, Joshi PA, Lai ES, Gujar P, Joubert L- M, Chen B, et al. Bilayered vascular graft derived from human induced pluripotent stem cells with biomimetic structure and function. Regenerative medicine. 2015;10(06):745–55. [PubMed: 26440211]
35. Lai ES, Huang NF, Cooke JP, Fuller GG. Aligned nanofibrillar collagen regulates endothelial organization and migration. Regenerative medicine. 2012;7(5):649–61. [PubMed: 22954436]
36. Islinger RB, Kuklo TR, McHale KA. A review of orthopedic injuries in three recent US military conflicts. Military medicine. 2000;165(6):463–5. [PubMed: 10870364]
37. McBride JT Jr, Hunt MM, Hannon JP, Hoxie SW, Rodkey W. Report and Medical Analyses of Personnel Injury from Operation'Just Cause'. LETTERMAN ARMY INST OF RESEARCH PRESIDIO OF SAN FRANCISCO CA; 1991.
38. Johnson BA, Carmack D, Neary M, Tenuta J, Chen J. Operation Iraqi freedom: the Landstuhl regional medical center experience. The Journal of foot and ankle surgery. 2005;44(3):177–83. [PubMed: 15940595]

39. Owens BD, Kragh JF Jr, Macaitis J, Svoboda SJ, Wenke JC. Characterization of extremity wounds in operation Iraqi freedom and operation enduring freedom. Journal of orthopaedic trauma. 2007;21(4):254–7. [PubMed: 17414553]
40. Nakayama KH, Surya VN, Gole M, Walker TW, Yang W, Lai ES, et al. Nanoscale Patterning of Extracellular Matrix Alters Endothelial Function under Shear Stress. Nano letters. 2016;16(1):410–9. [PubMed: 26670737]
41. Guex AG, Birrer DL, Fortunato G, Tevaearai HT, Giraud M-N. Anisotropically oriented electrospun matrices with an imprinted periodic micropattern: a new scaffold for engineered muscle constructs. Biomedical materials. 2013;8(2):021001. [PubMed: 23343525]
42. Kroehne V, Heschel I, Schügner F, Lasrich D, Bartsch J, Jockusch H. Use of a novel collagen matrix with oriented pore structure for muscle cell differentiation in cell culture and in grafts. Journal of cellular and molecular medicine. 2008;12(5a):1640–8. [PubMed: 18194451]
43. Corona BT, Garg K, Ward CL, McDaniel JS, Walters TJ, Rathbone CR. Autologous minced muscle grafts: a tissue engineering therapy for the volumetric loss of skeletal muscle. American Journal of Physiology-Cell Physiology. 2013;305(7):C761–C75. [PubMed: 23885064]
44. Ward CL, Pollot BE, Goldman SM, Greising SM, Wenke JC, Corona BT. Autologous minced muscle grafts improve muscle strength in a porcine model of volumetric muscle loss injury. Journal of orthopaedic trauma. 2016;30(12):e396–e403. [PubMed: 27466826]
45. Baker HB, Passipieri JA, Siriwardane M, Ellenburg MD, Vadhavkar M, Bergman CR, et al. Cell and Growth Factor-Loaded Keratin Hydrogels for Treatment of Volumetric Muscle Loss in a Mouse Model. Tissue Engineering Part A. 2017;23(11-12):572–84. [PubMed: 28162053]
46. Nindl BC, Santtila M, Vaara J, Hakkinen K, Kyrolainen H. Circulating IGF-I is associated with fitness and health outcomes in a population of 846 young healthy men. Growth Hormone & IGF Research. 2011;21(3):124–8. [PubMed: 21459641]
47. Adams GR, McCue SA. Localized infusion of IGF-I results in skeletal muscle hypertrophy in rats. Journal of Applied Physiology. 1998;84(5):1716–22. [PubMed: 9572822]
48. Cheema U, Brown R, Mudera V, Yang SY, McGrouther G, Goldspink G. Mechanical signals and IGF-I gene splicing in vitro in relation to development of skeletal muscle. Journal of cellular physiology. 2005;202(1):67–75. [PubMed: 15389530]
49. Sandonà D, Desaphy J- F, Camerino GM, Bianchini E, Ciciliot S, Danieli-Betto D, et al. Adaptation of mouse skeletal muscle to long-term microgravity in the MDS mission. PloS one. 2012;7(3).
50. Borselli C, Storrie H, Benesch-Lee F, Shvartsman D, Cezar C, Lichtman JW, et al. Functional muscle regeneration with combined delivery of angiogenesis and myogenesis factors. Proceedings of the National Academy of Sciences. 2010;107(8):3287–92.
51. Ruvinov E, Leor J, Cohen S. The promotion of myocardial repair by the sequential delivery of IGF-1 and HGF from an injectable alginate biomaterial in a model of acute myocardial infarction. Biomaterials. 2011;32(2):565–78. [PubMed: 20889201]
52. Hammers DW, Sarathy A, Pham CB, Drinnan CT, Farrar RP, Suggs LJ. Controlled release of IGF-I from a biodegradable matrix improves functional recovery of skeletal muscle from ischemia/reperfusion. Biotechnol Bioeng. 2012;109(4):1051–9. [PubMed: 22095096]
53. Rabinovsky ED, Draghia-Akli R. Insulin-like growth factor I plasmid therapy promotes in vivo angiogenesis. Molecular Therapy. 2004;9(1):46–55. [PubMed: 14741777]
54. Bloor CM. Angiogenesis during exercise and training. Angiogenesis. 2005;8(3):263–71. [PubMed: 16328159]
55. Gustafsson T, Puntschart A, Kaijser L, Jansson E, Sundberg CJ. Exercise-induced expression of angiogenesis-related transcription and growth factors in human skeletal muscle. American Journal of Physiology-Heart and Circulatory Physiology. 1999;276(2):H679–H85.
56. Saffari TM, Bedar M, Hundepool CA, Bishop AT, Shin AY. The role of vascularization in nerve regeneration of nerve graft. Neural Regeneration Research. 2020;15(9):1573. [PubMed: 32209756]
57. Petrella JK, Kim J-s, Mayhew DL, Cross JM, Bamman MM. Potent myofiber hypertrophy during resistance training in humans is associated with satellite cell-mediated myonuclear addition: a cluster analysis. Journal of Applied Physiology. 2008;104(6):1736–42. [PubMed: 18436694]

58. Joanisse S, Nederveen JP, Baker JM, Snijders T, Iacono C, Parise G. Exercise conditioning in old mice improves skeletal muscle regeneration. The FASEB Journal. 2016;30(9):3256–68. [PubMed: 27306336]

59. Inoue A, Cheng XW, Huang Z, Hu L, Kikuchi R, Jiang H, et al. Exercise restores muscle stem cell mobilization, regenerative capacity and muscle metabolic alterations via adiponectin/AdipoR1 activation in SAMP10 mice. Journal of cachexia, sarcopenia and muscle. 2017;8(3):370–85.

60. Hyldahl RD, Olson T, Welling T, Groscost L, Parcell AC. Satellite cell activity is differentially affected by contraction mode in human muscle following a work-matched bout of exercise. Frontiers in Physiology. 2014;5(485).

61. Bush JA, Blog GL, Kang J, Faigenbaum AD, Ratamess NA. Effects of Quadriceps Strength After Static and Dynamic Whole-Body Vibration Exercise. The Journal of Strength & Conditioning Research. 2015;29(5):1367–77. [PubMed: 25268289]

62. Kraemer R, Durand R, Acevedo E, Johnson L, Kraemer G, Hebert E, et al. Rigorous running increases growth hormone and insulin-like growth factor-I without altering ghrelin. Experimental Biology and Medicine. 2004;229(3):240–6. [PubMed: 14988516]

63. Jenkins PJ. Growth hormone and exercise. Clinical endocrinology. 1999;50(6):683–9. [PubMed: 10468938]

64. Nishida Y, Matsubara T, Tobina T, Shindo M, Tokuyama K, Tanaka K, et al. Effect of Low-Intensity Aerobic Exercise on Insulin-Like Growth Factor-I and Insulin-Like Growth Factor-Binding Proteins in Healthy Men. International Journal of Endocrinology. 2010;2010:452820. [PubMed: 20885914]

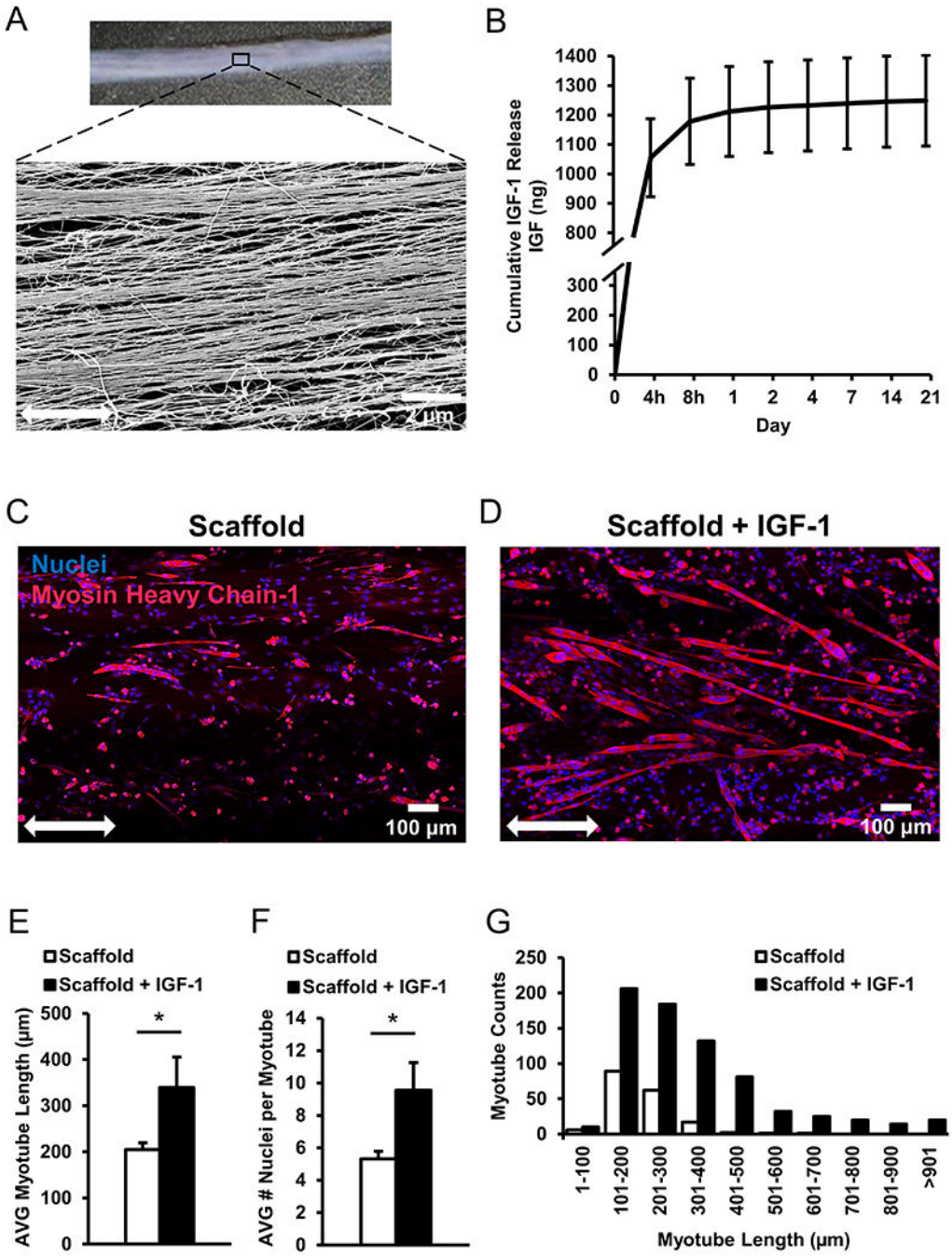

Figure 1.

Characterization and quantification of cellular interactions on IGF-1 laden scaffolds. **(A)** Low magnification image of 3D collagen scaffold with SEM expansion to show aligned nanofiber organization within the scaffold. **(B)** Release of IGF-1 from scaffolds laden with IGF-1 over a 21-day period measured by ELISA. **(C, D)** Immunofluorescence staining of C2C12 myoblasts seeded on scaffolds, without IGF-1 and with IGF-1, respectively. Double headed arrow denotes orientation of aligned nanofibers. **(E)** The average length of MHC^{+} myotubes containing nuclei ≥3 (n=4). **(F)** Quantification of the average number of nuclei per

myotube. **(G)** Distribution of myotube lengths on scaffolds represented in panels C & D, with and without IGF-1. * denotes a statistically significant relationship ($p<0.05$).

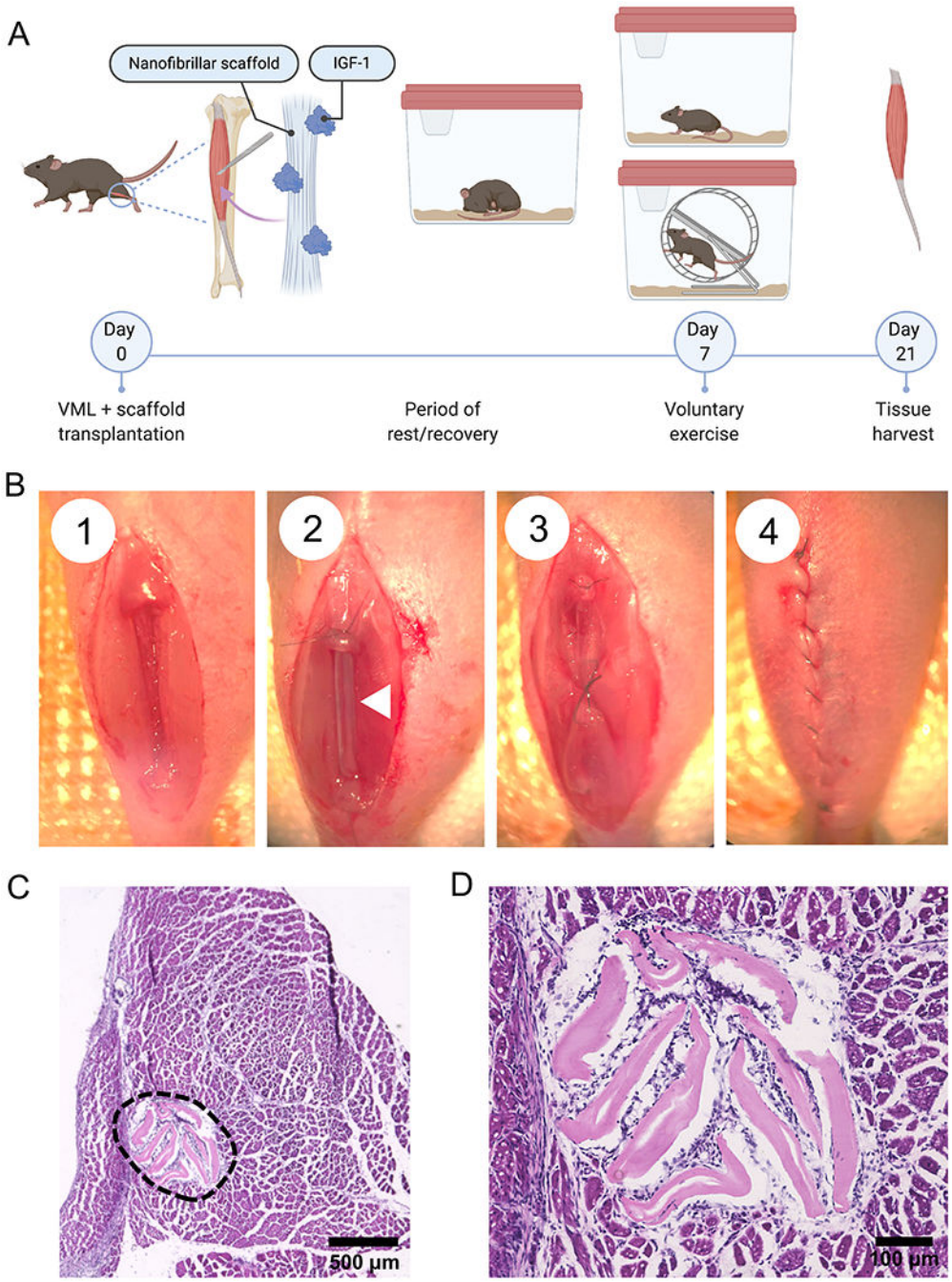

Figure 2.

Volumetric muscle loss in a murine model with voluntary exercise. **(A)** Schematic overview of the experimental design depicting induction of VML, introduction of voluntary running wheel exercise, and collection of tissues for histological analysis. **(B)** VML surgical procedure depicting (1) 20% muscle ablation, (2) scaffold implantation with scaffold denoted by white arrow, (3) muscle closure over the implanted scaffold and (4) skin incision closure with vicryl suture. **(C)** Hematoxylin and eosin (H&E) staining of transverse cross section of the tibialis anterior (TA) muscle with collagen scaffold implant (denoted by the

black dashed line), and **(D)** High magnification view of the scaffold implant from panel C to closely visualize the scaffold morphology within the muscle bundles 21 days after implant.

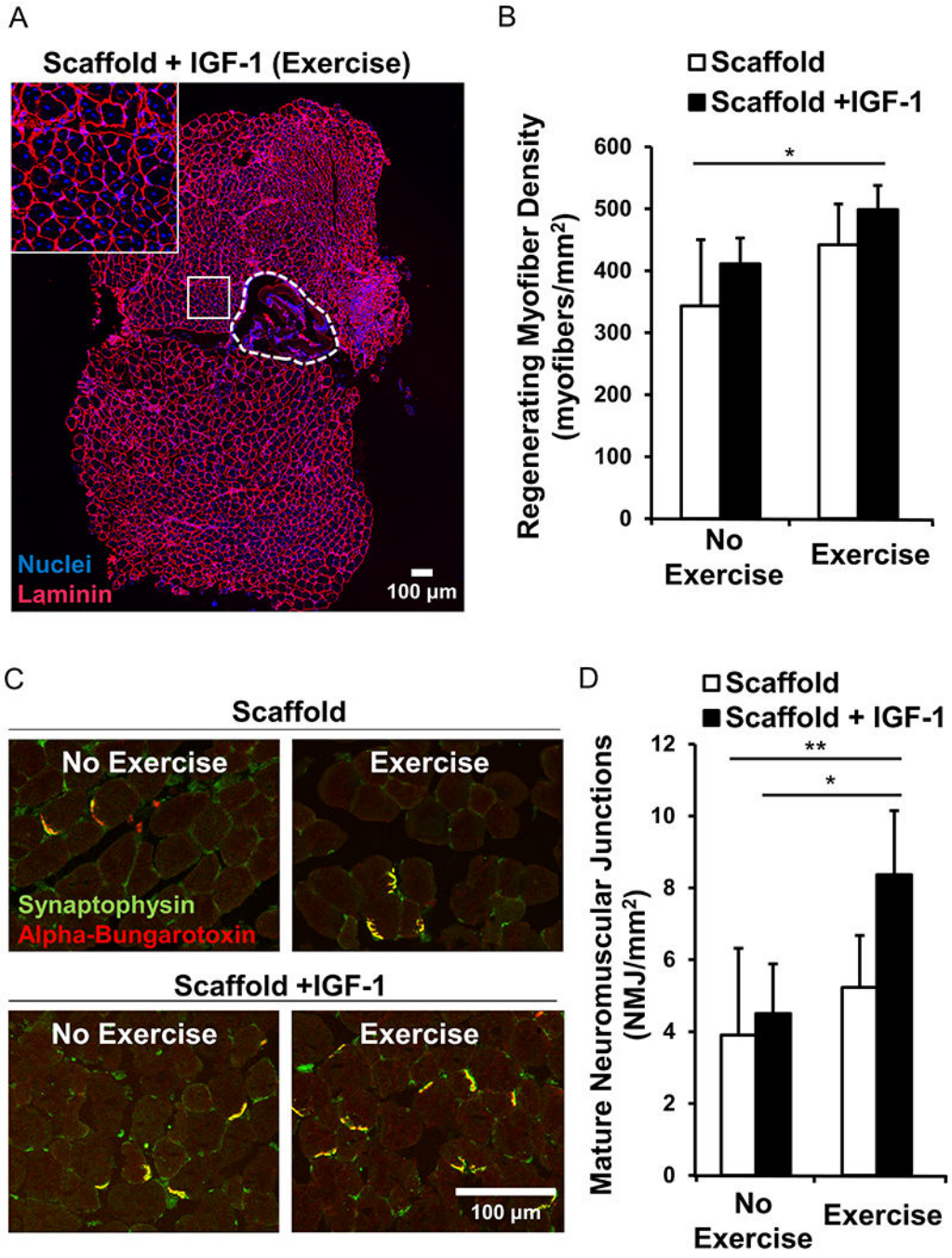

Figure 3.

Myofiber regeneration and tissue revascularization in the TA muscle. **(A)** Confocal microscopy of a representative transverse cross section of the TA muscle 21 days following injury and scaffold +IGF-1 implantation. Immunofluorescence staining of laminin used to delineate myofiber boundaries. Inset: Regenerating myofibers with centrally located nuclei adjacent to the scaffold (outlined by dashed white line) **(B)** Quantification of regenerating myofibers located within a 500 μm area from the scaffold region. **(C)** Immunofluorescence staining of mature neuromuscular junctions co-stained with synaptophysin+/alpha-

bungarotoxin+. **(D)** Quantification of mature neuromuscular junctions within a 500 μm radial area from the scaffold region. (n=4 for each group except n=6 for the scaffold+IGF-1 with exercise). * denotes a statistically significant relationship ($p<0.05$) and ** ($p<0.01$).

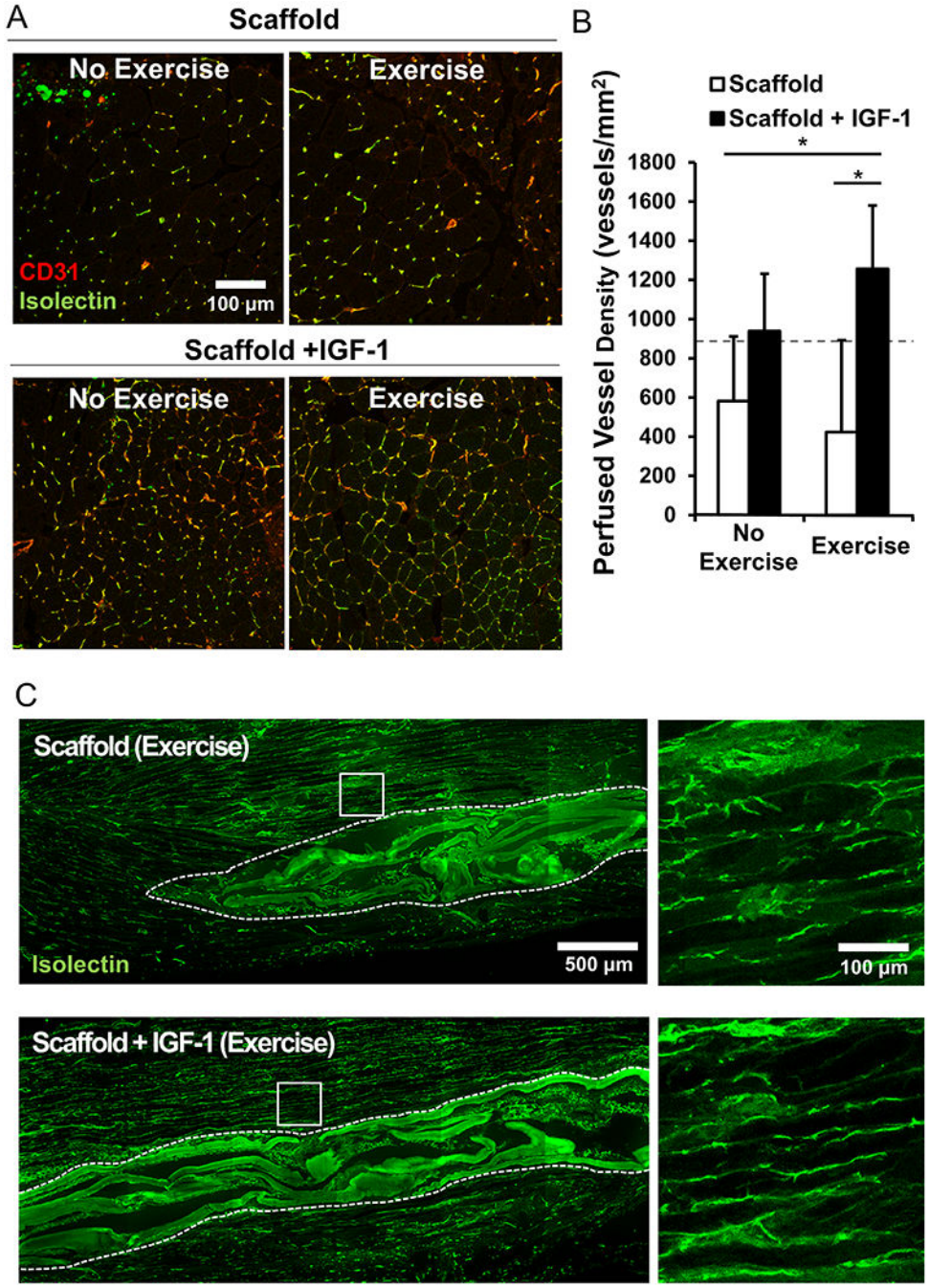

Figure 4.

Vessel regeneration and perfusion. **(A)** Immunofluorescence staining of co-stained CD31+/ Isolectin+ anastomotic vessels in the TA muscle **(B)** Quantified density of perfused vessels within a 500 μm area from the scaffold region. Dotted line represents control non-regenerating tissue values **(C)** Characterize of the vascular network along the myofiber bundles using immunofluorescence staining of Isolectin perfused vessels in longitudinal

muscle fibers adjacent to scaffold implant. (n=4 for each group except n=6 for the scaffold +IGF-1 with exercise). * denotes a statistically significant relationship ($p<0.05$).